Molecular Motors Govern Liquidlike Ordering and Fusion Dynamics of Bacterial Colonies

Anton Welker,* Tom Cronenberg,* Robert Zöllner,* Claudia Meel, Katja Siewering, Niklas Bender, Marc Hennes, Enno R. Oldewurtel, and Berenike Maier
Institute for Biological Physics, University of Cologne, Zülpicher Straße 77, 50937 Köln, Germany

(Received 4 October 2017; revised manuscript received 9 June 2018; published 11 September 2018)

Bacteria can adjust the structure of colonies and biofilms to enhance their survival rate under external stress. Here, we explore the link between bacterial interaction forces and colony structure. We show that the activity of extracellular pilus motors enhances local ordering and accelerates fusion dynamics of bacterial colonies. The radial distribution function of mature colonies shows local fluidlike order. The degree and dynamics of ordering are dependent on motor activity. At a larger scale, the fusion dynamics of two colonies shows liquidlike behavior whereby motor activity strongly affects surface tension and viscosity.

DOI: 10.1103/PhysRevLett.121.118102

Cocci are spherically shaped bacterial cells. Often, they produce surface structures that mediate attractive interactions between bacteria. Spheres with attractive interactions are reminiscent of nonliving colloidal systems with attractive interactions that tend to form liquid- or crystal-like structures. Assembly of colloidal crystals can be well controlled, e.g., by DNA hybridization or through electrostatic interactions [1–3]. Thereby, dynamics and efficiency of equilibration are very sensitive to the form and range of interaction potentials that are difficult to control experimentally [1,4].

In contrast to nonliving colloidal systems, bacterial cocci reproduce. During reproduction, their shape changes from spherical to dumbbell shaped. Another important difference of nonliving colloids is the use of attractive surface appendages with molecular motor properties. It is currently unclear how motor activity affects the structure of bacterial colonies. Here, *Neisseria gonorrhoeae* (gonococcus) and its type IV pilus (T4P) motors serve as a model system for addressing these questions. The gonococcus has a spherical cell body with a diameter of $\sim 0.7\ \mu$m. The extracellular T4P polymers are randomly located across the cell surface [5,6]. T4P act as depolymerization motors; as T4P polymers depolymerize, they retract and this retraction process can generate forces exceeding $F > 100$ pN onto a load attached to the pilus [7]. Pilus retraction is powered by the retraction ATPase PilT located at the base of the T4P machine (Fig. S1) [5,8,9]. When individual cells are attached to surfaces, multiple T4P cooperate for persistent movement through a tug-of-war mechanism [10,11]. When piliated bacteria are in close proximity to each other, T4P-T4P interactions induce self-assembly into colonies [12]. Self-assembly is reversible in young colonies [13]. Because deletion of T4P reduces the attractive interactions below the detection limit for gonococci [14,15], mutant strains in T4P-related genes provide a toolbox for tuning bacteria-bacteria interaction forces.

In this Letter, we test the hypothesis that spherical bacteria behave like a hard-sphere liquid with genetically tunable interactions. In our system, attractive interactions between bacteria are governed by the T4P motor. We show that molecular motor activity accelerates local liquidlike ordering and shape relaxations during colony fusion. Taken together, our results directly link molecular and macroscopic parameters by correlating interbacterial forces and binding probabilities with the spatiotemporal dynamics and materials properties of bacterial colonies.

Colonies show liquidlike order.—First, we investigated whether bacteria showed short-range order within colonies. To this end, wt* (Table S1 [9]) bacteria were incubated within a flow chamber under continuous nutrient supply for 6 and 24 h, respectively. Subsequently, the colony structures were imaged using confocal microscopy using *gfp*- and *mcherry*-expressing strains as described in Table S1 [9] and Refs. [16–22]. The dominant morphologies were spherical colonies (Fig. S2). A particle tracker was used to determine the three-dimensional coordinates of the cell bodies within the colonies (Figs. 1 and S3), as described in the Supplemental Material [9], which includes Refs. [23–25]. The bacteria were tightly packed within the colonies and the average density (number of nearest neighbors n within 1.4 μm of reference bacterium) tended to increase between 6 and 24 h of colony growth [Figs. 1(b), 1(c), and S3(d)]. Within some colonies, holes were present after 24 h. Therefore, we calculated the remoteness [26], i.e., the probability of having a distance r from each voxel to the centroid of the closest bacterium [Fig. S3(c)]. We found that the remoteness shifted to higher values after 24 h, in agreement with having more and larger areas that were not occupied with bacteria within the colony.

To address the question whether bacteria are ordered within the colonies, we determined the radial distribution function $g(r)$. $g(r)$ is defined so that $N/Vg(r)r^2dr$ is the

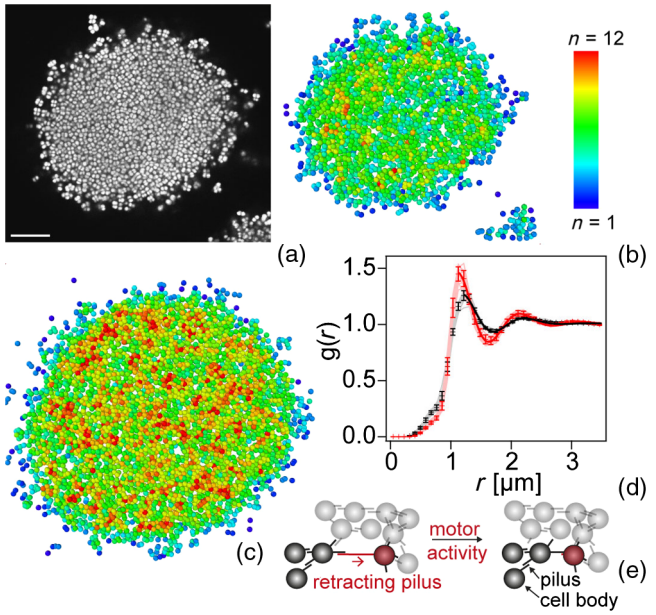

FIG. 1. (a) Confocal section of gonococcal wt∗ (Ng150) microcolony after 6 h. Reconstruction of 2 μm slices of bacterial coordinates after (b) 6 and (c) 24 h of growth. The colors encode the number of nearest neighbors n. (d) Radial distribution functions $g(r)$ after 6 h (black) and 24 h (red). Shaded lines: $g(r)$ of individual colonies. Full line: fit to Eq. (1). Dots and error bars: mean and standard deviation of 15 colonies from three independent experiments. Scale bar: 10 μm. (e) Hypothetical sketch of how T4P retraction supports local ordering.

probability that the center of a bacterium will be found in the range dr at a distance r from the center of another bacterium, where N/V is the number density of bacteria. At 6 h, $g(r)$ showed two maxima [Fig. 1(d)]. At higher cell-to-cell distances, the distribution is flat, indicating that no order existed at a distance exceeding $r = 2.5$ μm or three cellular diameters. After 24 h, the position of the first maximum shifted to a lower value. A lower average contact distance is in agreement with increased cell density and agrees well with Fig. S3(d) and Figs. 1(b) and 1(c), showing an increase in the number of nearest-neighbor cells. Moreover, the peaks became more pronounced, indicating stronger ordering. The shapes of $g(r)$ show good qualitative agreement with individual-based simulations that explicitly take T4P dynamics into account [27]. They are also reminiscent of the radial distribution functions found in colloidal systems with Lennard-Jones-like interactions [28]. Various analytical expressions for $g(r)$ have been proposed for Lennard-Jones fluids and shown to fit the radial distribution function obtained from Monte Carlo simulations very well [29,30]. Here, we used the formula proposed by Matteoli and Mansoori [29],

$$g(r > r_0) = 1 + y^{-m}[g(r_0) - 1 - \lambda] + \left(\frac{y - 1 + \lambda}{y}\right) \times \exp[-\alpha(y-1)]\cos[\beta(y-1)], \quad (1)$$

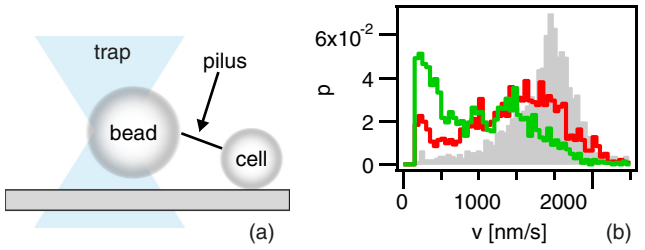

FIG. 2. Tuning T4P motor dynamics. (a) Experimental setup for characterizing the velocity of pilus retraction. (b) Velocity distribution of T4P retraction for force clamped at $F = 30$ pN. Gray: wt∗ (Ng170); red: $pilT_{WB1}$ (Ng171); green: $pilT_{WB2}$ (Ng176).

where r_0 is the contact distance between two bacteria, $y = r/r_0$, and m, λ, α, and β are adjustable parameters (Table S2 [9]). In particular, the contact distance was found to decrease from $r_0^{6h} = (1.18 \pm 0.02)$ to $r_0^{24h} = (1.14 \pm 0.01)$ μm and the amplitude of the first maximum increased from $g(r_0)^{6h} = 1.23 \pm 0.02$ to $g(r_0)^{24h} = 1.46 \pm 0.02$. To summarize, gonococcal colonies show increasing local ordering and density with time.

Nonfunctional T4P retraction ATPases affect pilus motor activity.—Attractive force between gonococci is primarily generated by type IV pili [13,14]. Deletion of these hairlike appendages inhibits the formation of colonies. Here, we addressed the question whether local ordering required motor activity of the T4P. The idea is that T4P form a network between the bacteria, and retraction of individual T4P generates a tug of war between bacteria [Fig. 1(e)], causing local order. To scrutinize this idea, we used a mutant strain lacking the T4P retraction ATPase PilT. These bacteria generate pili capable of supporting colony formation. However, pili cannot retract and therefore active force generation is inhibited in this strain [31]. For tuning motor activities, we additionally generated strains $pilT_{WB1}$ and $pilT_{WB2}$, where we introduced nonfunctional $pilT_{WB}$ under the control of different promoters in addition to functional $pilT$. The rationale behind this construction was that nonfunctional $\mathrm{PilT_{WB}}$ is likely to exert a dominant-negative effect on T4P retraction because PilT functions as hexamers that induce T4P retraction upon binding to the T4P complex [32]. Using a bacteria-two hybrid approach, we verified that the interaction between PilT-PilT and PilT-$\mathrm{PilT_{WB}}$ was comparable (Fig. S6 [9]), strongly suggesting that PilT-$\mathrm{PilT_{WB}}$ heterohexamers form.

We used our previously established T4P retraction assay for quantifying the effect of the $pilT_{WB}$ expression on motor activity [Fig. 2(a)] [10,33]. The distribution of T4P retraction velocities shifted to lower values in strain $pilT_{WB1}$ compared to wt∗ and to even lower values for strain $pilT_{WB2}$ [Fig. 2(b)]. In the presence of nonfunctional $\mathrm{PilT_{WB}}$, the probability of finding a T4P in the state of elongation or pausing increased in strains $pilT_{WB1}$ and $pilT_{WB2}$ (Fig. S7 [9]). In conclusion, expression of nonfunctional $pilT_{WB}$ ATPases strongly affects T4P motor

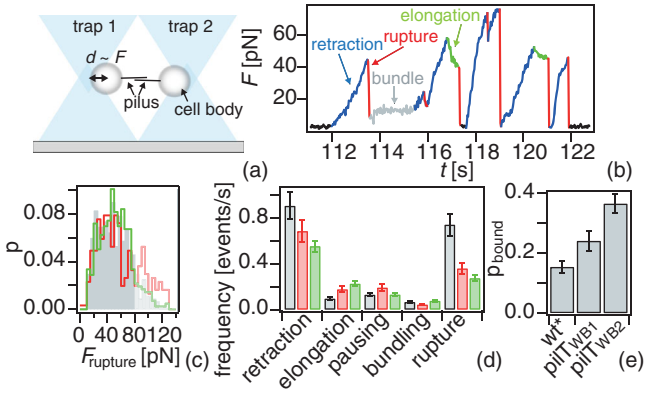

FIG. 3. Tuning bacterial interaction dynamics. (a) Experimental setup. A spherical cell is trapped in each of two laser traps. The deflection d of the cell body from the center of the trap yields the force acting on both cell bodies $F \sim d$. When pili of both cells bind to each other and one of them retracts, both cell bodies are pulled towards each other. (b) Typical force F as a function of time t. (c) Distribution of rupture forces for gray: wt∗ (Ng170); red: $pilT_{WB1}$ (Ng171); green: $pilT_{WB2}$ (Ng176). Forces were measurable up to 80 pN. ($N > 300$ for each strain). (d) Frequencies of T4P retraction, elongation, pausing, bundling, and rupture. Color codes as in (c). $N = 38$–844 per strain and condition; error bars: bootstrapping with $N = 100$. (e) Probability that at least one pair of pili from different cells are attached to each other. Error bars: bootstrapping.

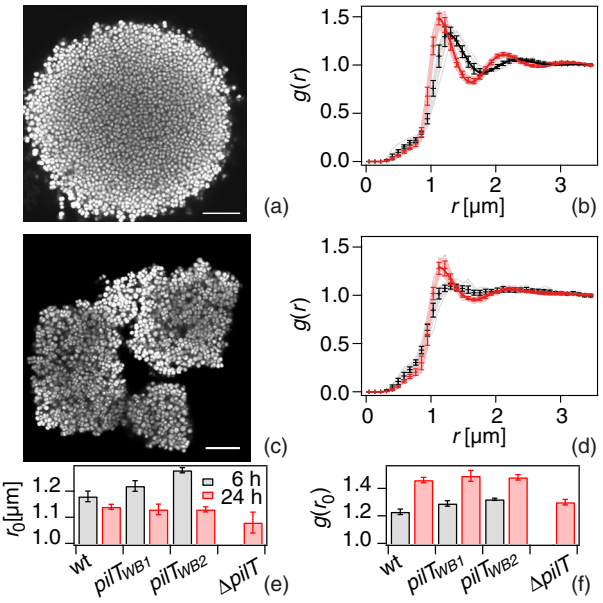

FIG. 4. (a) Typical confocal section after 6 h and (b) radial distribution functions $g(r)$ of T4P retraction reduced $pilT_{WB2}$ (Ng176) microcolony after 6 h (black) and 24 h (red). (c) Typical confocal section after 6 h and (d) radial distribution functions $g(r)$ of T4P retraction inhibited $\Delta pilT$ (Ng178) microcolony after 6 h (black) and 24 h (red). Shaded lines: $g(r)$ of individual colonies. Full line: fit to Eq. (1). Dots and error bars: mean and standard deviation of at least 15 colonies from three independent experiments. Scale bar: 10 μm. (e) Contact distance r_0 and (f) value of radial distribution function at r_0 obtained from fit to Eq. (1).

activity, namely, motor velocity and the probability of finding the motor in the states of retraction, elongation, and pausing, respectively.

Pilus motor activity affects bacterial interactions.—We aimed at correlating changes in motor activity with changes of the interactions between bacteria. We used a dual laser trap setup for characterizing the dynamics of pilus-mediated interaction forces between two bacteria [Fig. 3(a)]. The setup is described in the Supplemental Material [9,34]. A spherical bacterium was trapped within each of the laser traps. When the pili from different bacteria bind to each other and at least one of them retracts, the bacteria are attracted towards each other [Fig. 3(b)]. We observed different states of pilus-pilus interactions including T4P retraction pulling both bacteria towards each other, elongation, where the bacteria moved away from each other, and pausing, where d was constant but nonzero. Often, bacteria moved away from each other at a rate larger than 10 μm/s, indicating that the bond between pili had ruptured. Sometimes, the cell did not return to the center of the laser trap after a rupture event. In this case (denoted as bundling), we assume that more than one pilus was bound and while the shortest bond had ruptured, the second shortest bond kept the bacteria deflected from the center of the trap. The mean rupture force was $F^{\mathrm{wt}*}_{\mathrm{rupture}} = (50 \pm 24)$ pN for wt∗ [Fig. 3(c)]. Neither strain $pilT_{WB1}$ nor strain $pilT_{WB2}$ showed significantly different distributions (Kolmogorow-Smirnow test) from the wt∗ distribution. Next, we investigated the frequencies at which the transitions to a specific state occurred [Fig. 3(d)]. The frequency at which T4P retracted decreased in the presence of nonfunctional $PilT_{WB}$, while the frequency of elongations increased. Importantly, the rupture frequency decreased in the presence of $PilT_{WB}$. The probability that two cells in the laser traps were connected through pili increased in strain $pilT_{WB1}$ and was highest in strain $pilT_{WB2}$ [Fig. 3(e)]. This observation can be explained by the effect of $PilT_{WB}$ on motor activity. T4P tend to elongate rather than detach (Fig. S7 [9]) favoring T4P-T4P binding. Additionally, since the detachment rate is force dependent [10] and the velocity of T4P retraction is lower [Fig. 2(b)], the probability of finding T4P attached to each other increases. Taken together, the newly designed strains allow us to tune the dynamics of pilus-mediated attraction through T4P retraction and the frequencies at which pili detach and thus release the interaction between adjacent cells.

Active motors accelerate local ordering.—The structures of the colonies formed by strains $pilT_{WB1}$ and $pilT_{WB2}$ were very similar to the wt∗ structure [Figs. 4(a), 4(b), and S8]. Interestingly, after 6 h, the contact distances of these mutant strains were larger compared to the contact distance of the wt∗ [Figs. 4(e) and 4(f)]. After 24 h, both the contact distance $r_0^{WB2,24h} = (1.13 \pm 0.01)$ μm and the

amplitude of the first maximum $g(r_0)^{WB2,24h} = 1.48 \pm 0.02$ were comparable to the wt∗ parameters. When T4P retraction was fully inhibited by deleting *PilT*, both the local and the global colony structure were very different from the wt∗ structure [Figs. 4(c), 4(d), and S9]. The shape of microcolonies formed by Δ*pilT* cells was nonspherical in agreement with previous studies [12,35]. The cell density was lower compared to wt∗ colonies (Fig. S9). After 6 h of growth, $g(r)$ showed no evidence for local order [Fig. 4(d)], indicating that active T4P retraction accelerated the process of local liquidlike ordering. After 24 h, a maximum became discernible, although its amplitude was lower compared to the wt∗ amplitude with $r_0^{\Delta pilT,24h} = (1.08 \pm 0.04)\ \mu$m and $g(r_0)^{\Delta pilT,24h} = 1.30 \pm 0.02$. In summary, active force generation by T4P is not essential for local liquidlike ordering, but it enhances the rate at which local order and dense cellular packaging are achieved.

Motor activity governs shape relaxations.—We addressed the question whether T4P-mediated interaction forces supported liquidlike behavior of bacterial colonies at length scales beyond a few bacterial diameters. Like liquids, populations of self-attracting cocci form spherical colonies that coalesce upon contact [12,13]. We tested whether the dynamics of colony fusion were in agreement with the shape changes exhibited by an initially ellipsoidal liquid drop as it minimizes its surface area. Using the mutant strains expressing nonfunctional $pilT_{WB}$, we can tune the molecular interactions between the bacteria and investigate their effect on the macroscopic properties. During the fusion process, we assume that the energy change due to the reduction of surface area is balanced by the work of viscous deformation. We used the following fluid model of fusion dynamics to describe the shape changes during the fusion of two colonies [36,37]. Let the initial shape of the fusing colony be described by an oblate ellipsoid with the ratio of the minor axis b and major axis a, $f = b/a$, and its volume $v = 4/3\pi ab^2$. Then the rate of deformation of the drop is

$$\frac{df}{dt} = \frac{\sigma}{v^{1/3}\eta}\rho(f), \tag{2}$$

where σ is the surface tension and η is the viscosity. $\rho(f)$ is described in the Supplemental Material [9]. If at time t_0 an ellipsoid of cells has an axial ratio f_0 and by time t it reaches f, then

$$v^{\frac{1}{3}}[\tau(f_1) - \tau(f_0)] = \frac{\sigma}{\eta}[t_1 - t_0]. \tag{3}$$

τ can be obtained by numerical integration of $\rho(f)$.

Experiments were initiated by inducing disassembly of colonies by oxygen depletion, as described before [13]. Subsequently, oxygen-rich medium was applied, triggering the formation of motile colonies [Fig. 5(a)]. Once two colonies converged, they fused into a single colony whose projection in the xy plane took the shape of an ellipse. Figure 5(b) shows that $v^{1/3}[\tau(f) - \tau(f_0)]$ increases linearly with time in agreement with the dynamics predicted for the fusion of two highly viscous liquid drops [Fig. 5(b)]. The dynamics of shape changes was slower for the $pilT_{WB1}$ strain compared to the wt∗ strain and the distribution of the ratio between surface tension and viscosity σ/η was shifted to lower values [Fig. 5(c)]. For describing the short term dynamics of fusion, we used a different model describing the "neck" length of two fusing colonies as a function of time [38] (Fig. S10 [9]). At short timescales on the order of 10 s, the shapes relax faster than the model predicts. At longer timescales, the relaxation dynamics is well described by the model and σ/η agrees with Fig. 5(c). We propose that the relaxation dynamics at short times is dominated by a layer of motile cells residing at colony surfaces [14].

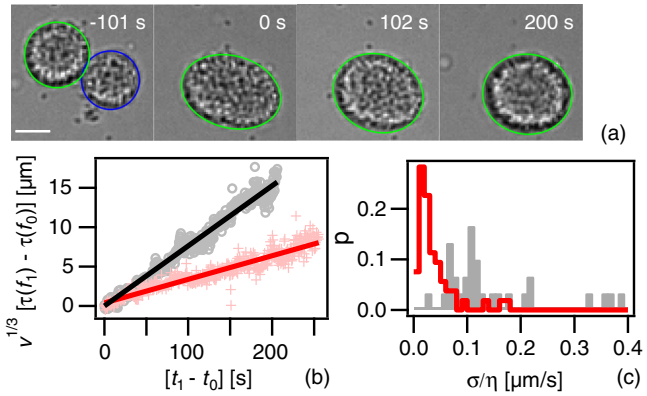

FIG. 5. (a) Time lapse of wt∗ colony fusion event. (b) Typical $v^{1/3}[\tau(f) - \tau(f_0 = 0.71)]$ as a function of time. Gray circles: wt∗ (Ng151); red crosses: $pilT_{WB1}$ (Ng171). Full lines: fits to Eq. (3). (c) Distribution of ratio between surface tension σ and viscosity η obtained from Eq. (3). Gray: wt∗ (Ng151); red: $pilT_{WB1}$ (Ng171). $N > 30$ colonies.

Next, we relate the materials property σ/η to the molecular interactions characterized in Fig. 3. Taking into account the rupture force F_{rupture}, the average number of pili per cell [6], and the probability that two cells are bound p_{bound} through pilus-pilus interaction, we estimate the surface tension σ (Supplemental Material [9]) and obtain $\sigma_{\text{wt}*} \approx 5 \times 10^{-5}$ and $\sigma_{WB1} \approx 8 \times 10^{-5}$ Nm^{-1}. Experimentally, we confirmed the right order of magnitude by deforming colonies through centrifugation (Fig. S11) [39–41]. Using these values, our experimentally determined ratios of σ/η (Fig. 5) yield the viscosities of $\eta_{\text{wt}^*} \approx 350$ and $\eta_{WB1} \approx 2000$ N s m^{-2}. The increased probability of pilus-pilus binding in the $pilT_{WB1}$ strain is consistent with a lower off rate and explains increased viscosity. Using computer simulations, Pönisch *et al.* showed that the shape relaxation strongly depends on T4P-T4P rupture force and detachment times [27]. Using rupture forces comparable to our experimental system

(Fig. 3), they found liquidlike dynamics of shape relaxation in very good agreement with our experiments. Very recently, Bonazzi *et al.* measured the viscosity in a related bacterial system, namely, noncapsulated *Neisseria meningitidis* [42]. Using micropipette aspiration, they found a value of $\eta_{\mathrm{Nm}} = 50\ \mathrm{N\,sm^{-2}}$, somewhat lower than our value. Remarkably, colonies formed by capsulated (wt) *N. meningitidis* have considerably lower viscosity and higher surface tension compared to *N. gonorrhoeae* studied here. Together with our results on systematic variations of motor properties, this shows that fine-tuning T4P dynamics and binding kinetics has a tremendous effect on the material properties of the colonies. In summary, the fusion dynamics of gonococcal colonies are in good agreement with the dynamics of shape changes expected during fusion of liquid drops, whereby surface tension and viscosity are determined by the motor properties of the pili.

Conclusion.—We have shown that motor activity of T4P accelerates the processes of local ordering and shape relaxation during colony fusion. Our bacterial mutants allowed us to tune the frequency of T4P retractions and the detachment times between T4P of adjacent cells. This is most consistent with a role of T4P in increasing the attachment and/or detachment dynamics between bacteria, accelerating the "equilibration" of the colony structure. For DNA-directed assembly, strong interactions tended to support fractal structures or small aggregates reminiscent of our force-deficient $\Delta pilT$ aggregates [1] (Fig. 4). We suggest that in our system cellular reproduction inhibits crystalline ordering because dumbbell formation before cell division introduces polydispersity and asymmetric cell shapes. Taken together, motor activity of T4P accelerates dense packing of bacteria, possibly allowing bacteria to protect themselves when facing external stress, including antibiotic treatment or the prohibitive action of probiotic bacteria.

We thank Nadzeya Kouzel, Katja Henseler, and Andrea Höne for experimental support, Katrina Forest and Michael Koomey for providing us with antibodies, the CECAD imaging facility of support with confocal microscopy, Kazem Edmont, Roel Dullens, Jan Dhont, and Stefan Egelhaaf for help with image analysis, Ramin Golestanian for helpful discussions, and the Deutsche Forschungsgemeinschaft and the Human Frontiers in Science Project for funding through Grants No. MA3898 and No. RGP0061.

[*] These authors contributed equally to this work.

[1] P. L. Biancaniello, A. J. Kim, and J. C. Crocker, Phys. Rev. Lett. **94**, 058302 (2005).
[2] M. P. Valignat, O. Theodoly, J. C. Crocker, W. B. Russel, and P. M. Chaikin, Proc. Natl. Acad. Sci. U.S.A. **102**, 4225 (2005).
[3] E. Spruijt, H. E. Bakker, T. E. Kodger, J. Sprakel, M. A. C. Stuart, and J. van der Gucht, Soft Matter **7**, 8281 (2011).
[4] A. J. Kim, R. Scarlett, P. L. Biancaniello, T. Sinno, and J. C. Crocker, Nat. Mater. **8**, 52 (2009).
[5] B. Maier and G. C. L. Wong, Trends Microbiol. **23**, 775 (2015).
[6] C. Holz, D. Opitz, L. Greune, R. Kurre, M. Koomey, M. A. Schmidt, and B. Maier, Phys. Rev. Lett. **104**, 178104 (2010).
[7] B. Maier, L. Potter, M. So, H. S. Seifert, and M. P. Sheetz, Proc. Natl. Acad. Sci. U.S.A. **99**, 16012 (2002).
[8] R. Kurre, N. Kouzel, K. Ramakrishnan, E. R. Oldewurtel, and B. Maier, PLoS One **8**, e67718 (2013).
[9] See Supplemental Material at http://link.aps.org/supplemental/10.1103/PhysRevLett.121.118102 for details of materials and methods, bacterial strain descriptions, supplementary figures, and supplementary tables.
[10] R. Marathe *et al.*, Nat. Commun. **5**, 3759 (2014).
[11] V. Zaburdaev, N. Biais, M. Schmiedeberg, J. Eriksson, A. B. Jonsson, M. P. Sheetz, and D. A. Weitz, Biophys. J. **107**, 1523 (2014).
[12] D. L. Higashi, S. W. Lee, A. Snyder, N. J. Weyand, A. Bakke, and M. So, Infect. Immun. **75**, 4743 (2007).
[13] L. Dewenter, T. E. Volkmann, and B. Maier, Integr. Biol. **7**, 1161 (2015).
[14] E. R. Oldewurtel, N. Kouzel, L. Dewenter, K. Henseler, and B. Maier, eLife **4**, e10811 (2015).
[15] R. Zollner, E. R. Oldewurtel, N. Kouzel, and B. Maier, Sci. Rep. **7**, 12151 (2017).
[16] N. Kouzel, E. R. Oldewurtel, and B. Maier, J. Bacteriol. **197**, 2422 (2015).
[17] T. Tonjum, N. E. Freitag, E. Namork, and M. Koomey, Mol. Microbiol. **16**, 451 (1995).
[18] R. Kurre, A. Hone, M. Clausen, C. Meel, and B. Maier, Mol. Microbiol. **86**, 857 (2012).
[19] M. Wolfgang, P. Lauer, H. S. Park, L. Brossay, J. Hebert, and M. Koomey, Mol. Microbiol. **29**, 321 (1998).
[20] F. E. Aas, H. C. Winther-Larsen, M. Wolfgang, S. Frye, C. Lovold, N. Roos, J. P. van Putten, and M. Koomey, Mol. Microbiol. **63**, 69 (2007).
[21] J. M. Koomey and S. Falkow, J. Bacteriol. **169**, 790 (1987).
[22] L. A. Cahoon and H. S. Seifert, Science **325**, 764 (2009).
[23] X. Gao and M. L. Kilfoil, Opt. Express **17**, 4685 (2009).
[24] J. C. Crocker and D. G. Grier, J. Colloid Interface Sci. **179**, 298 (1996).
[25] M. Allen and D. Tildesley, *Computer Simulation of Liquids* (Claredon Press, Oxford, 1991).
[26] J. Hendricks, R. Capellmann, A. B. Schofield, S. U. Egelhaaf, and M. Laurati, Phys. Rev. E **91**, 032308 (2015).
[27] W. Pönisch, C. A. Weber, G. Juckeland, N. Biais, and V. Zaburdaev, New J. Phys. **19**, 015003 (2017).
[28] P. Atkins and J. de Paula, *Physical Chemistry*, 10th ed. (Oxford University Press, New York, 2014).
[29] E. Matteoli and G. A. Mansoori, J. Chem. Phys. **103**, 4672 (1995).
[30] M. Bamdad, S. Alavi, B. Najafi, and E. Keshavarzi, Chem. Phys. **325**, 554 (2006).
[31] A. J. Merz, M. So, and M. P. Sheetz, Nature (London) **407**, 98 (2000).
[32] A. M. Misic, K. A. Satyshur, and K. T. Forest, J. Mol. Biol. **400**, 1011 (2010).

[33] M. Clausen, M. Koomey, and B. Maier, Biophys. J. **96**, 1169 (2009).
[34] D. Opitz and B. Maier, PLoS One **6**, e17088 (2011).
[35] A. M. Hockenberry, D. M. Hutchens, A. Agellon, and M. So, mBio **7**, e01994 (2016).
[36] R. Grima and S. Schnell, Dev. Biol. **307**, 248 (2007).
[37] R. Gordon, L. L. Wiseman, M. S. Steinberg, and N. S. Goel, J. Theor. Biol. **37**, 43 (1972).
[38] E. Flenner, L. Janosi, B. Barz, A. Neagu, G. Forgacs, and I. Kosztin, Phys. Rev. E **85**, 031907 (2012).
[39] A. Kalantarian, H. Ninomiya, S. M. Saad, R. David, R. Winklbauer, and A. W. Neumann, Biophys. J. **96**, 1606 (2009).
[40] V. A. Lubarda and K. A. Talke, Langmuir **27**, 10705 (2011).
[41] M. Godin *et al.*, Nat. Methods **7**, 387 (2010).
[42] D. Bonazzi *et al.*, Cell **174**, 143 (2018).